Remote Sensing of Environment 130 (2013) 245–253

Contents lists available at SciVerse ScienceDirect

Remote Sensing of Environment

journal homepage: www.elsevier.com/locate/rse

Tradeoffs between lidar pulse density and forest measurement accuracy

Marek K. Jakubowski [a], Qinghua Guo [b], Maggi Kelly [a,*]

[a] Department of Environmental Science, Policy, and Management, 130 Mulford Hall #3114, University of California, Berkeley, CA 94720-3110, USA
[b] School of Engineering, 5200 North Lake Rd., University of California, Merced, Merced, CA 95343, USA

ARTICLE INFO

Article history:
Received 11 June 2012
Received in revised form 19 November 2012
Accepted 23 November 2012
Available online 29 December 2012

Keywords:
Lidar
Pulse density
Machine learning
Gaussian processes
Sierra Nevada forests
Forest structure

ABSTRACT

Discrete airborne lidar is increasingly used to analyze forest structure. Technological improvements in lidar sensors have led to the acquisition of increasingly high pulse densities, possibly reflecting the assumption that higher densities will yield better results. In this study, we systematically investigated the relationship between pulse density and the ability to predict several commonly used forest measures and metrics at the plot scale. The accuracy of predicted metrics was largely invariant to changes in pulse density at moderate to high densities. In particular, correlations between metrics such as tree height, diameter at breast height, shrub height and total basal area were relatively unaffected until pulse densities dropped below 1 pulse/m^2. Metrics pertaining to coverage, such as canopy cover, tree density and shrub cover were more sensitive to changes in pulse density, although in some cases high prediction accuracy was still possible at lower densities. Our findings did not depend on the type of predictive algorithm used, although we found that support vector regression (SVR) and Gaussian processes (GP) consistently outperformed multiple regression across a range of pulse densities. Further, we found that SVR yielded higher accuracies at low densities (<0.3 pl/m^2), while GP was better at high densities (>1 pl/m^2). Our results suggest that low-density lidar data may be capable of estimating typical forest structure metrics reliably in some situations. These results provide practical guidance to forest ecologists and land managers who are faced with tradeoff in price, quality and coverage, when planning new lidar data acquisition.

1. Introduction

The use of airborne lidar in forest studies has been on the rise in the last decade as increasing numbers of researchers use these data to predict directly measurable canopy characteristics (e.g. tree height, shrub height, etc.) as well as derived metrics (e.g. total basal area, biomass, carbon inventory, etc.) (Wulder et al., 2008). Since airborne lidar acquisition over large areas is costly, lidar missions necessarily involve tradeoffs. Researchers must decide between cost and coverage; between cost and lidar pulse density, between density and coverage; and at the same time maintain accuracy. Practical questions arise for scientists and managers using lidar to map forests: how large an area can I cover with a set budget? What is the minimum lidar pulse density that I can use and still get accurate results? In this paper, we first consider the tradeoffs between cost, coverage and lidar pulse density, and then describe an experiment that directly examines the relationship between density and accuracy for various forest structure metrics at plot scale.

1.1. The cost of lidar

From a cost perspective, lidar is a viable option for remote sensing forest analysis. Lidar can already be less expensive or comparable to image data analysis when the entire cost of research (data acquisition, analysis, personnel, software, etc.) is considered, especially for large areas (Johansen et al., 2010). Johansen et al. (2010) analyzed 26,000 km of a stream network using three datasets: lidar (3.98 pt/m^2), QuickBird imagery, and SPOT-5 imagery; the total research cost using these three approaches were approximately $3.8 M, $6.4 M, and $2.6 M (Australian dollars), respectively. Tilley et al. (2004) also reported economies of scale; costs per ha declined from $37/ha to approximately $1/ha for large areal coverage (400 km^2).

Acquisition costs are related to coverage and lidar pulse density[1] (Baltsavias, 1999; Lovell et al., 2005), although the precise relationship between these variables is difficult to determine as most studies do not report cost. Higher pulse densities can be obtained by independently increasing the pulse rate frequency (PRF), scanning rate, flight

* Corresponding author. Tel.: +1 5106427272.
E-mail addresses: marek@berkeley.edu (M.K. Jakubowski), qguo@ucmerced.edu (Q. Guo), maggi@berkeley.edu (M. Kelly).

[1] Lidar pulse density is discussed in the literature in many ways, often with *pulses*, *points*, *returns*, and *echoes* used interchangeably. In this work, we define a *pulse* ("pl") as the laser signal sent out from the lidar system towards the ground. A *point* ("pt"), also referred to as a return or an echo, is the signal, or multiple signals, reflected from target(s) back towards the lidar system (e.g. up to four points can be recorded from each pulse sent out by a typical lidar system).

0034-4257/$ – see front matter © 2012 Elsevier Inc. All rights reserved.
http://dx.doi.org/10.1016/j.rse.2012.11.024

path overlap (or repeated flights), or by decreasing the flight altitude or the aircraft speed. Ultimately, the pulse density is related to the time that the aircraft/sensor spends flying, which translates to direct effect on acquisition costs. As a result of the tradeoffs between cost, coverage and density, land managers of vast areas (e.g. national forests) must often decide between ordering a low pulse density data that covers a large area or a higher pulse density data that concentrates on a subsection of their forest. Fig. 1 conceptually illustrates the decision space for managers with a fixed amount to spend, or with a fixed target area. The cost per-square-area decreases as the study area increases. For example, managers with a constant budget (horizontal line) could afford a slightly larger area at 7 pl/m^2 and a much larger area at 1 pl/m^2 when compared to 9 pl/m^2.

1.2. Is high-density data necessary?

An important question to this work is whether high-density data are necessary to obtain accurate results in plot-scale lidar forestry. As technology improves, there has been a trend to acquire data at increasingly higher densities, reflecting the belief that this will improve accuracies. Researchers have speculated that higher pulse densities could improve the delineation of individual trees (Brandtberg et al., 2003), the derivation of elevation and tree heights (Clark et al., 2004), as well as predominant height and LAI (Lovell et al., 2003).

However, lidar data were not always gathered at high densities. A number of early lidar studies reported relatively high measures of correlation between lidar and field data using low-density data (<1 pl/m^2). Hodgson and Bresnahan (2004) derived a digital elevation model (DEM) and validated the elevation error to be below 25.9 cm using 0.25 pt/m^2 data. Takahashi et al. (2010) derived stand volume and estimated a 10–39% root-mean squared error (RMSE) at $r^2 = 0.75$ using variable pulse density data between 0.125 and 0.25 pt/m^2. In one case, Thomas et al. (2006) has reported that using lower (0.035 pt/m^2) rather than higher (4 pt/m^2) lidar density resulted in higher correlation coefficients when predicting canopy metrics. Although the difference was small, they found that 8 out of the 11 tested metrics improved (root total biomass, stem bark, stem wood, foliage and all tree height metrics), root basal area remained the same, while only crown closure and live branches decreased in accuracy with the lower density data.

Further, in large projects, lidar data are often acquired at low pulse densities. The ongoing initiative to obtain nationwide lidar data for the continental United States is one example. In a few states the acquisition has already begun or has been completed. For example, Louisiana collected lidar data at 0.06–0.11 pt/m^2 (Cunningham et al., 2004), Ohio at 0.04–1 pt/m^2, and Iowa at 0.11 pt/m^2 (Veneziano et al., 2002). These efforts are targeted at the creation of digital elevation models (DEM), and thus the densities are much lower than typical forest research lidar data acquisitions (1–9 pl/m^2). The relevant question that we address here is whether this already-collected low-density data could yield sufficiently high accuracies to reliably predict forest structure metrics *in addition* to DEMs.

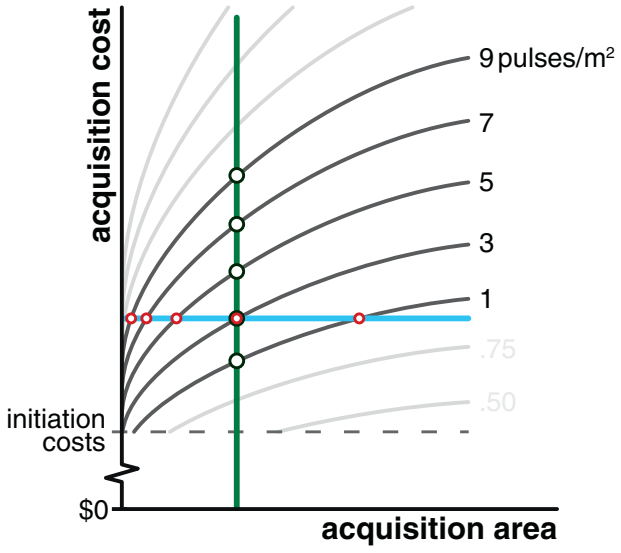

Fig. 1. Conceptual diagram of tradeoffs between cost, data density, and area surveyed. The light blue, horizontal line represents decision space for managers with a fixed amount to spend: the area they can cover will increase with decreasing densities. The dark green line represents decision space for managers with a fixed target area: the price of collection will increase with pulse density. The cost of all pulse densities starts at a significant initial cost (mobilization of the aircraft, mission planning, etc.). The rate at which price increases for a larger study area decreases, i.e. cost per-square-area decreases as the study area increases. Using this logic, a constant budget (horizontal line) could afford a slightly larger area at 7 pl/m^2 and a much larger area at 1 pl/m^2 when compared to 9 pl/m^2.

1.3. Density and accuracy

The tradeoff between lidar pulse density and accuracy has been examined in several ways. Several researchers have investigated this experimentally by collecting data at multiple flying heights (i.e. above ground level or AGL); in general they found that AGL has little or no effect on the accuracy of predictions. Goodwin et al. (2006) analyzed the accuracy of the generated DEM, tree height, crown area, and tree volume, and found that with the exception of individual tree extraction, the predictions exhibited little to no effect based on the sensor altitudes—1000, 2000, and 3000 m AGL. Takahashi et al. (2010) reported similar results at three altitudes—500, 1000, and 1500 m AGL—with very high and simulated low pulse densities—57, 25, and 9 pl/m^2 and 0.25–0.125 pl/m^2, respectively. In an earlier study, they found that increasing the AGL decreases penetration and intensity with little effect on accuracy (Takahashi et al., 2008). Thomas et al. (2006) found higher AGL/lower density yielded slightly better results, while Næsset (2004) found no significant effect on stand height, volume, or basal area when comparing the same pulse density obtained at two AGLs.

Several studies considered the effect of lidar point (not pulse) density on the accuracy of predicted products. However, most of these studies concentrate on the accuracy of a generated DEM. Although many use dissimilar measures for quantifying the accuracy, most of the studies agree that the error increases exponentially as the point spacing increases. This is true across topographic spectrum: in flat sites using low (Anderson et al., 2006) and medium pulse density (Olsen et al., 2009), in low-relief or undulating hills at various elevations (Goodwin et al., 2006; Liu & Zhang, 2008; Sanii, 2008), and in steep, mountainous terrain using medium (Olsen et al., 2009) to high pulse density data (Guo et al., 2010; Pirotti & Tarolli, 2010).

In the few studies that examined canopy metrics the results are more variable. When considering tree height and/or volume, research has found little increase in accuracy as a function of point density, whether simulated (Tesfamichael et al., 2010), or collected at different altitudes (Goodwin et al., 2006; Takahashi et al., 2010), unless the densities are simulated at very low levels (0.004 p/m^2) in which case the error grows exponentially (Magnusson et al., 2007). Pulse density *does* affect individual tree detection, however, as reported by Takahashi et al. (2010) and Goodwin et al. (2006). Similarly, stream network extraction becomes problematic at high pulse spacing (Pirotti & Tarolli, 2010). However, while these studies are informative, they typically do not realistically simulate lower density data as though they were collected by a multiple-return lidar sensor at a higher AGL or lower PRF. Instead, the original data are typically thinned by even percentages (e.g. 75, 50, and 25% of the original point cloud) (Anderson et al., 2006; Guo et al., 2010; Liu & Zhang, 2008; Olsen et al., 2009; Pirotti & Tarolli, 2010). Such results are not easily

used by new researchers or land mangers that must determine the appropriate pulse density for their new lidar acquisitions.

In this study, we simulate how predictions of various forest canopy and understory metrics vary with lidar pulse density. Our objective was to determine the lowest pulse density that enables derivation of forest structure metrics at the plot scale at an acceptable accuracy level. We report all findings in terms of the simulated pulse density—the typically-used specification when ordering lidar data. This practical and realistic approach yields results that are important not only to the scientific lidar community but also for land managers making decisions about lidar data acquisition parameters. Our results will enable land managers to more reliably predict canopy metrics of interest with lidar data, while maximizing the coverage area given a set budget.

2. Materials and methods

This is a comprehensive study of the effect of lidar pulse density on extraction of various canopy and shrub metrics in the range from 0.01 to 9 pl/m^2. We extracted ten forest structure metrics that cover the vertical profile of a forest stand: maximum and mean tree height, total basal area, tree density, mean height to live crown base (HTLCB), canopy cover, maximum and mean diameter at breast height (DBH), and shrub cover and height. To ensure that the visible effect is a result of pulse density and not a particular algorithm, we used three different approaches for canopy metric prediction: a simple multiple regression model, a support vector regression machine learning algorithm, and Gaussian processes.

2.1. Study area

Our study area is located in northern California, USA, in the Tahoe National Forest (39° 07′ N, 120° 36′ W) (Fig. 2). It spans over 9950 ha on topographically steep and complex terrain between 600 m and 2186 m above sea level. Since 1990, the average precipitation is 1182 mm/year. The study area is 93% forested according to the Tahoe National Forest definition (Collins et al., 2011). Tree-ring analysis indicates high-frequency (5–15 years), low-intensity fires (Stephens & Collins, 2004), which is consistent and expected in this mixed-conifer, Mediterranean-climate forest. The dominant species include red and white fir (*Abies magnifica* and *Abies concolor*), ponderosa pine (*Pinus ponderosa*), sugar pine (*Pinus lambertiana*), incense-cedar (*Calocedrus decurrens*), and California black oak (*Quercus kelloggii*). The majority of the area is managed by the United States Department of Agriculture, Forest Service, with a limited number of private inholdings.

2.2. Data

2.2.1. Field data

In this study we analyzed data from 248, 0.05 ha circular plots (radius = 12.62 m). The plot centers were regularly spaced at 500 m intervals at even UTM coordinates (e.g. 710500 m E, 4329000 m N; 710500 m E, 4329500 m N; etc.). The few plots that were physically inaccessible, intersected rivers, road surfaces, or landings, were offset by 25 m in random directions. The ground truth data were collected during 2007 and 2008 summer field seasons according to a rigorous field protocol previously described in Collins et al. (2011) and Jakubowski et al. (in press). In summary, all trees' height, DBH, species,

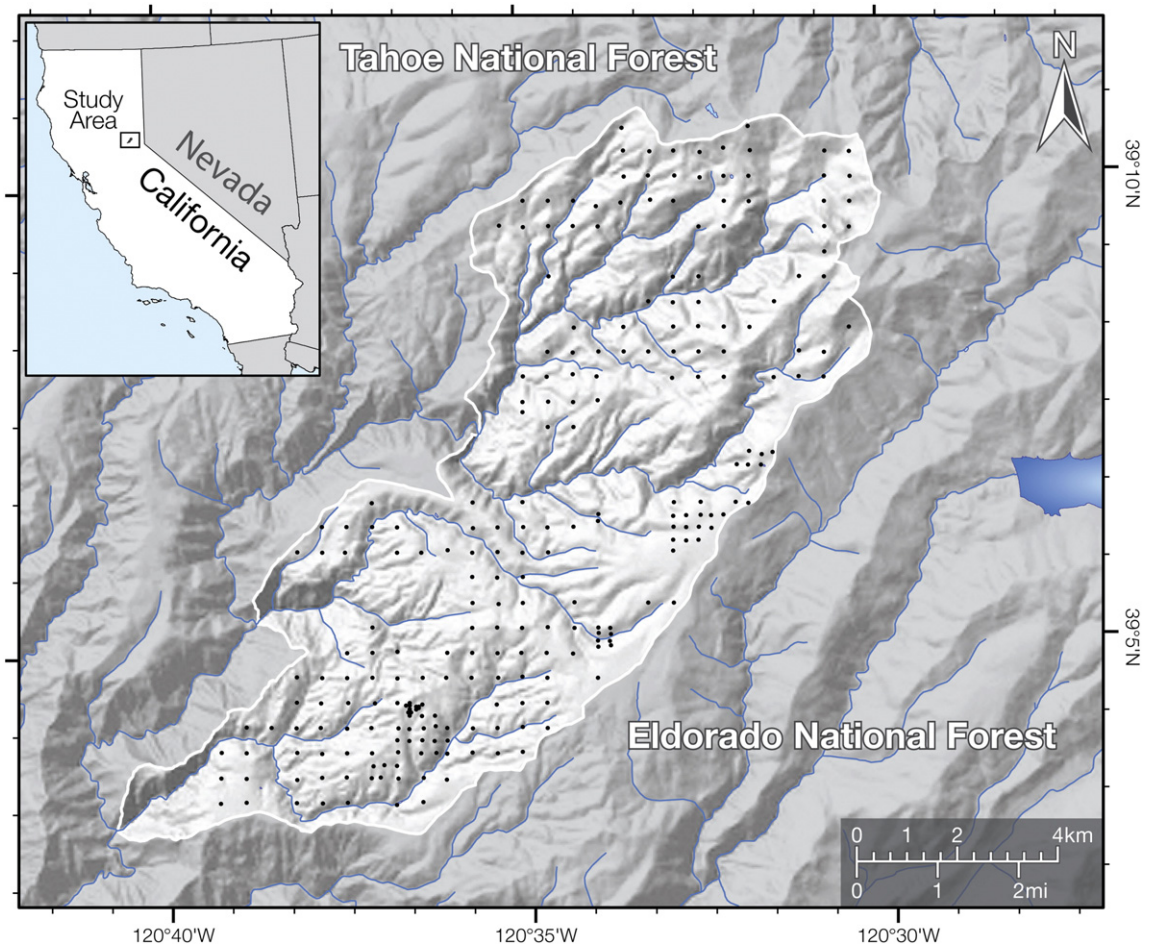

Fig. 2. The study area (9950 ha), mostly within Tahoe National Forest, is covered by mixed conifer forest, and covers topographically complex terrain.

and HTLCB were measured. We define HTLCB as the lowest extent of the live canopy; small trees below the canopy are included if there is no complete separation. All trees within the plot with DBH ≥ 19.5 cm were identified by a unique number. Smaller trees (5 ≤ DBH ≤ 19.5 cm) were measured on one third of each plot, designated by a random azimuth angle from north. A total of 7284 trees were used in this analysis, including 4581 with unique IDs and precise coordinates. The distributions of the trees' DBH and height are typical of a mixed-conifer Sierra Nevada forest. We also characterized the understory by measuring shrub percent cover, height, and species. Five photographs were captured (toward the plot center from north, east, south, and west of the plot, and directly up from the plot center) to help characterize the forest structure of the plots.

All plots were georeferenced using a spatial accuracy protocol. First, we find an optimal area to collected differential global positioning system (dGPS) signal-i.e. open canopy-ideally at or up to 30 m from the plot center. There, we position a Trimble Zephyr antenna elevated 3 m from the ground and attached to Trimble GeoXH GPS receiver. We record at least 300 (typically 1000, and up to 7000) measurements at positional dilution of precision (PDOP) < 5. The dGPS measurements are post-processed using data from Continuously Operating Reference Stations (CORS) and University NAVSTAR Consortium (UNAVCO) stations. All CORS and UNAVCO stations used in post-processing were less than 20 km from all field measurements. We use a combination of Impulse Laser Rangefinder, Impulse Electronic Compass, and a Trimble GeoXH receiver to georeference plot centers and tree locations. The rangefinder is placed between the GPS antenna and the plot, such that the laser distance measurement error (≤2 cm) and the compass degree error (≤0.5°) are minimized.

2.2.2. Lidar data

The lidar data were collected in five flights from September 19–21, 2008 (leaf-on conditions) at an average flying height of 950 m AGL. The acquisition area (10700 [[[comma placement inconsistent with the rest of the document]]] ha) was larger than the study area to ensure complete, high-density data coverage. An Optech GEMINI Airborne Laser Terrain Mapper (ALTM) was used by the National Center for Airborne Laser Mapping (NCALM) to collect all data. Up to 4 returns were recorded from each pulse. The lidar data were collected at a minimum of 6 and an average of 9 pl/m^2. Because of dense vegetation, the lidar system often recorded multiple returns with more than 20 pts/m^2. All data were processed, recorded, and delivered in the Universal Transverse Mercator (UTM) coordinate system in the 1983 North American Datum (NAD83) and the North American Vertical Datum of 1988 (NGS GEOID03 model).

2.3. Analysis

2.3.1. Lidar pre-processing

The raw lidar data were pre-processed before the outlined workflow (Fig. 3). In particular, the data provider, NCALM, used TerraSolid's TerraScan software (Soininen, 2012) to remove isolated, "air," and below-surface points. For example, isolated points were defined as those with no neighbors within 5 m. The point cloud was separated into above-ground and ground points using an iterative triangle-building surface model classification routine (Chang et al., 2008). All digital elevation models (DEM) were generated using inverse distance weighted interpolation as suggested by Guo et al. (2010).

2.3.2. Simulating lidar pulse densities

The data were reduced to 17 pulse densities: 9, 8, 7, 6, 5, 4, 3, 2, 1, 0.75, 0.50, 0.25, 0.10, 0.075, 0.040, 0.025, and 0.01 pl/m^2 (process illustrated in Fig. 4). There are a number of ways to simulate lower density data; for instance, Magnussen et al. (2010) used a static, 1 m moving window to randomly choose points from the point cloud to reach the desired point density. Because we wanted to simulate data obtained at specific pulse densities, our goal was to replicate the multiple-return effect as best as possible—in other words, sensor setting of x pulse/m^2 posting density will produce a point cloud with y points/m^2, where $y > x$. To simulate this process, the original lidar data were divided into 100 m square tiles, each centered at a ground-reference plot. From these square tiles, only the first return points were saved and their average point density was recorded. The first-return points are assumed to correspond to the number of pulses sent out, as at least first-returns are recorded from each originating pulse. An optimization script was developed in combination with *lasthin* from *lastools* (Isenburg, 2011) to calculate a correct thinning factor for each 100 m square tile (N = 248), at each pulse density. The thinning was achieved by gridding the lidar data at different spatial resolutions and then choosing a random point within each cell. 4216 files were processed this way to obtain 248 plot lidar point clouds at 17 different pulse densities. The reduced first-return point clouds were manually checked to ensure that proper pulse densities were obtained. Finally, the obtained thinning factors were used to reduce the original, all-return lidar data. This simulated lidar point clouds at multiple pulse densities with up to four returns per pulse.

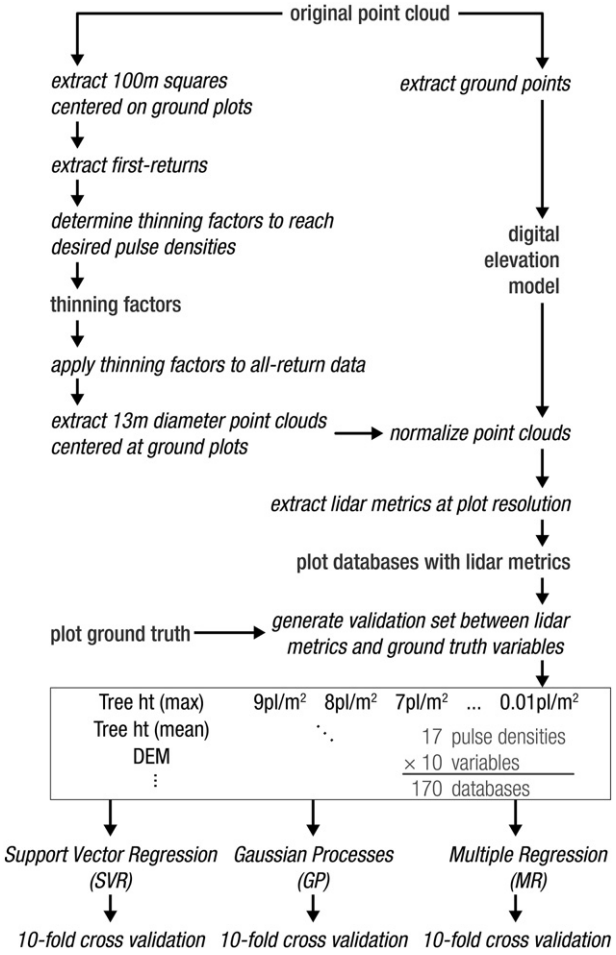

Fig. 3. Workflow used to derive all forest metrics.

2.3.3. Extraction of lidar metrics

From each 100 m square tile, we extracted all points within 13 horizontal meters of the plot center to match the plot's footprint. We used 13 m radius to account for any possible misalignment due to lidar or dGPS positional error. The 13 m horizontal radius point cloud was normalized by subtracting the DEM-derived elevation from each point's z-value yielding height above ground and removing any topographic effects. The point cloud is summarized by calculating descriptive statistics of the entire vertical profile (e.g. *mean height*,

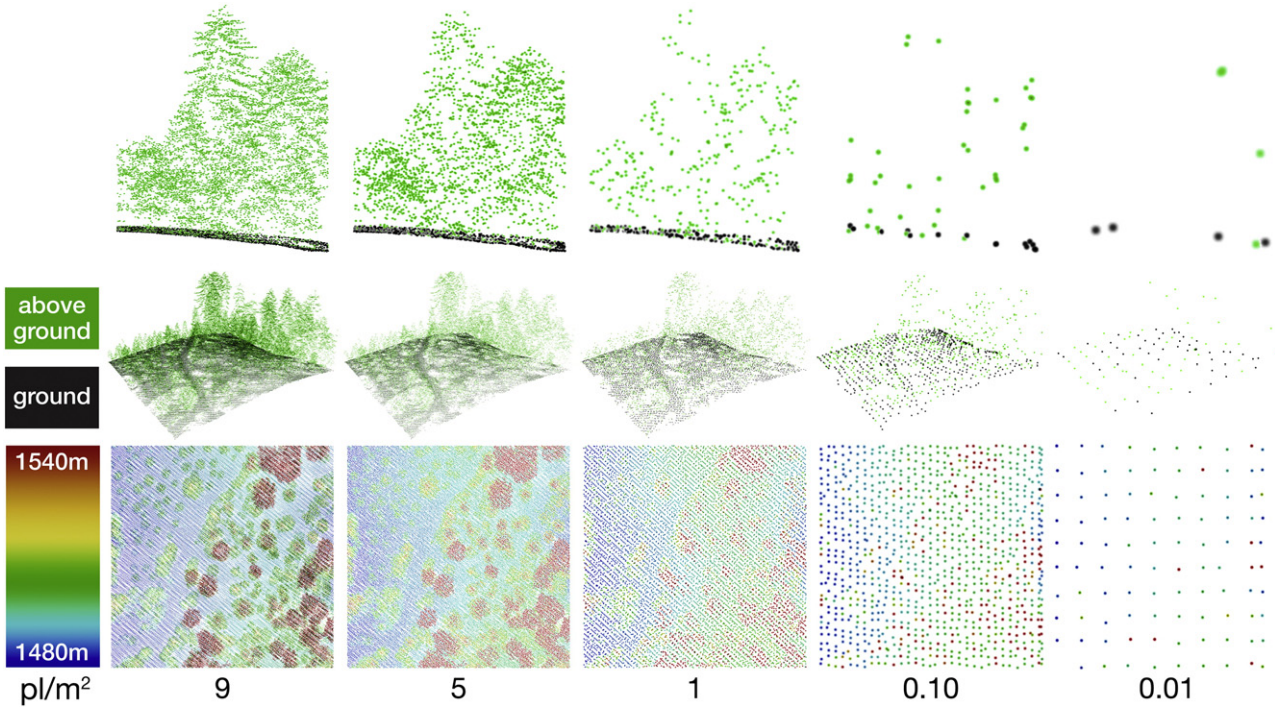

Fig. 4. Simulation of pulse densities (as indicated by the number of pulses/m^2). Only five out of the 17 simulated densities are shown here. The side and oblique, 3-D perspective (middle panel) shows the point cloud as classified into ground and above-ground points. In the bottom panel the same point clouds are visualized from above; the color corresponds to elevation of each point. The relative size of lidar points in lower density clouds is exaggerated for visual clarity.

percentiles, *standard deviation*, etc.) and point densities throughout the vertical column (e.g. *point density between 3 and 4 m above the ground*). The list of extracted metrics is provided in Table 1. Because the focus of this work was to compare accuracies obtained from various pulse densities, only the lidar points directly above the plots are considered in validation. The validation procedure described here is equivalent of deriving such products at a 26 m pixel size.

2.3.4. Forest structure prediction and validation

The lidar metrics described above were calculated for all plots, at all pulse densities, and then copied into a plot database. A series of files were generated-one for each forest metric and at all densities-to derive forest structure predictions and to cross-validate them. All lidar metrics were used in the prediction algorithms. We used Waikato Environment for Knowledge Analysis (WEKA) software (Frank et al., 2010), developed at University of Waikato, New Zealand to produce the results. WEKA is a software package designed to utilize various data mining algorithms. We use three example algorithms-a simple multiple regression (MR), support vector regression (SVR) with sequential minimal optimization (SMO), and Gaussian processes (GP)-to compare their performance and to ensure that the effect we see is a result of pulse density and not of using a particular validation method. The use of SVR and GP algorithms in forestry lidar has been successfully documented in the literature (Jakubowski et al. in press; Zhao et al., 2011).

Table 1
Descriptive and statistical metrics extracted from the lidar data. The point density voxels were extracted based on heights above the DEM.

Variables extracted from lidar	
Elevation	Point density: 0 to 0.5 m
Height: minimum	Point density: 0.5 to 1 m
Height: mean	Point density: 1 to 1.5 m
Height: maximum	Point density: 1.5 to 2 m
Height: standard deviation	Point density: 2 to 3 m
Total number of returns	Point density: 3 to 4 m
Quintile 0.01	Point density: 4 to 5 m
Quintile 0.05	Point density: 5 to 10 m
Quintile 0.10	Point density: 10 to 15 m
Quintile 0.25	Point density: 15 to 20 m
Quintile 0.50	Point density: 20 to 25 m
Quintile 0.75	Point density: 25 to 30 m
Quintile 0.90	Point density: 30 to 35 m
Quintile 0.95	Point density: 35 to 40 m
Quintile 0.99	Point density: 40 to 45 m
	Point density: 45 to 50 m
	Point density: 50 to 55 m
	Point density: 55 m and above

SVR algorithms use data points close to class boundaries (the support vectors) within feature space to fit a hyperplane to the training data (Keerthi et al., 2001). SVR methods are particularly suitable in high-dimensional datasets when the training sample size is small because only the data points closest to the hyperplane boundary are used (Hsu et al., 2003). There are many variations of the SVR algorithms; in this paper, we use the regression-based SMO implemented within WEKA, which uses a loss function to penalize errors that are greater than certain threshold on the training data (Frank et al., 2010; Keerthi et al., 2001; Smola & Schölkopf, 2004).

GP method is a robust, Bayesian method for non-parametric regression. A Gaussian process is a stochastic process for which any linear combination of samples has a joint Gaussian distribution. It is defined as a collection of random variables and can be described by its mean function—a vector—and a covariance function—a matrix (Rasmussen, 2004). GPs are appealing because they can model arbitrary functions (i.e. they are non-parametric), they yield simple linear algebra implementations, and the uncertainty of their predictions is quantifiable. We used WEKA's standard implementation of GP in this work.

Each algorithm was validated using a 10-fold validation procedure as suggested by Kohavi (1995). In addition, we calculated the RMSE for each predicted metric and at all pulse densities. Our final report consists of the average correlation coefficients and the range of the RMSE values for each relationship between the lidar data and a forest

structure and/or shrub metric, each as a function of pulse density. As an example, for tree height, we report the average correlation coefficient and RMSE between field data across all plots and lidar data at 17 densities using 3 different prediction algorithms.

3. Results and discussion

We extracted lidar metrics to analyze how pulse density affects prediction of various forest structure metrics. We evaluated ten forest variables across the vertical profile, at 17 pulse densities, using three different predictive models (MR, SVR, and GP), to ensure that the visible trends result from pulse density and not from using a particular algorithm. The 10-fold correlation coefficients based on cross-validation of the predicted values and the ground data are plotted in Fig. 5. All accuracies decreased as the pulse density approached 0.01 pl/m^2. The accuracies of some of the metrics remained relatively high until very low densities (in many cases up to about 1 pl/m^2). Similar trends were found by He and Li (2012) and Lovell et al. (2005), although the latter study digitally generated the entire point cloud and the forest environment to study these effects. He and Li (2012) analyzed lidar densities between 0.23 and 5.23 pt/m^2 to extract tree height and crown diameter in a Chinese, coniferous forest. The RMSE increased as the pulse density decreased in a similar pattern for all metrics. Because the RMSE trend was similar for all predictive models, we report the range of the errors instead of the individual values (Fig 6). We have identified a number of trends in the results, as described below.

In general, the relative overall accuracy of a forest metric was similar across all three predictive models. In all models, maximum tree height had the highest correlation coefficients followed by mean HTLCB and total basal area. The accuracy of the predicted forest structure metrics decreased roughly with its vertical position within the canopy; maximum tree height yielded highest accuracy, the accuracy declined for mean DBH, while shrub cover and height consistently produced the lowest accuracies.

The accuracy of the forest structure metrics increased as a function of pulse density at various rates. Further, each accuracy response line (Fig. 5) reaches a point at which the accuracy either levels off or approaches maximum accuracy (the “turning point” in the trend). These turning points and best accuracy results are summarized in Fig. 7. Collectively, these results indicate that beyond a certain density level, accuracy does not increase significantly.

The correlation coefficients of tree density and canopy cover increased significantly and consistently without a plateau from lowest to highest pulse densities (e.g. 0.271 to 0.753 at 0.01 and 9 pl/m^2 for tree density using GP, respectively). This indicates that maximum achievable accuracy of these two metrics may be beyond 9 pl/m^2. Others (maximum tree height and DBH metrics) significantly improved in accuracy within the lower pulse densities followed by consistent yet small increase. These are good examples of metrics that

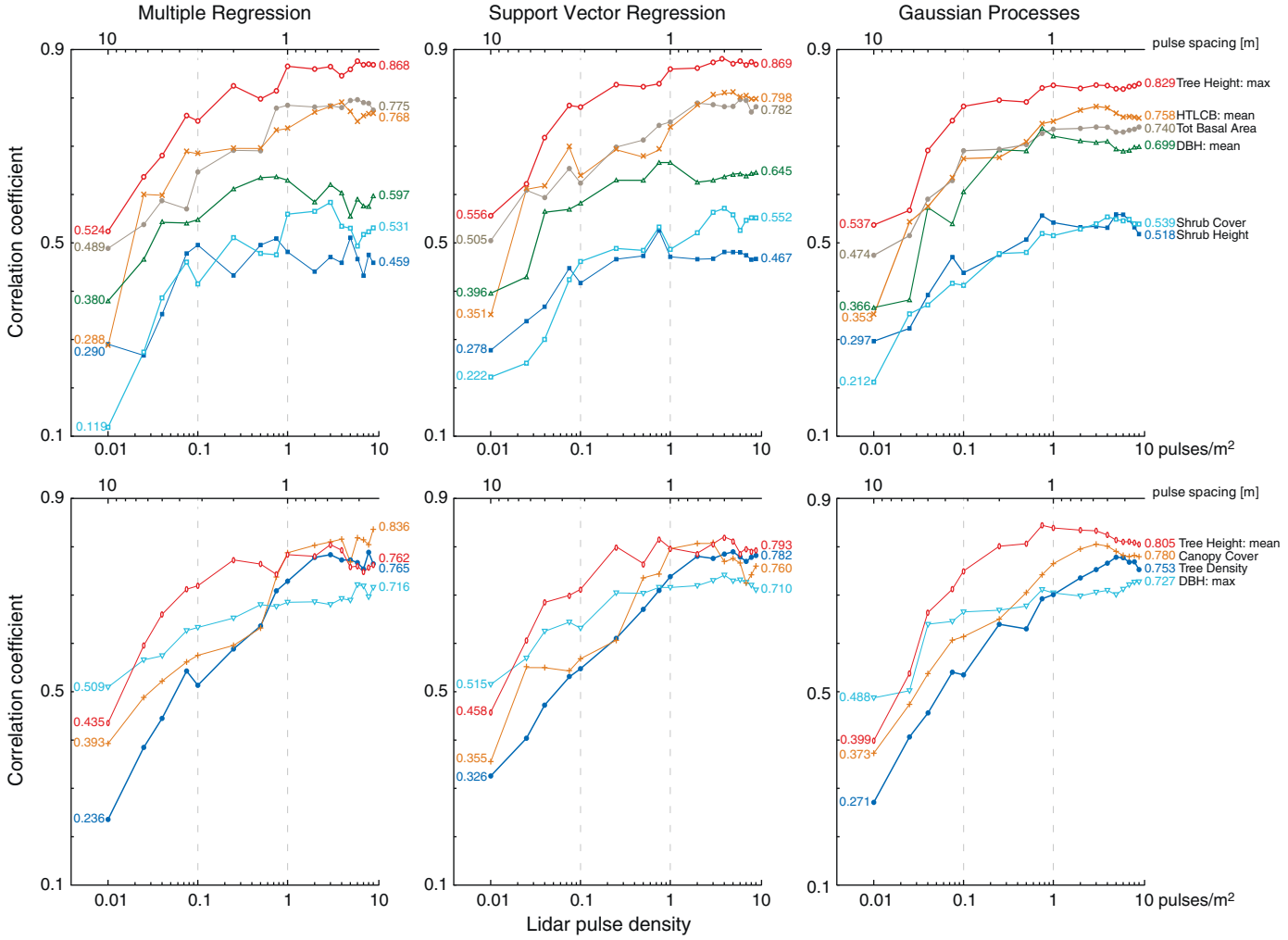

Fig. 5. Ten-fold, cross-validation correlation coefficients of a number of predicted forest structure metrics using three algorithms: MR, SVR, and GP. The results are plotted as a function of pulse density on a logarithmic scale. The coefficient values are provided for lowest and highest pulse densities. Pulse density is provided in number of pulses per square meter (bottom axes) as well as the equivalent pulse spacing (top axes).

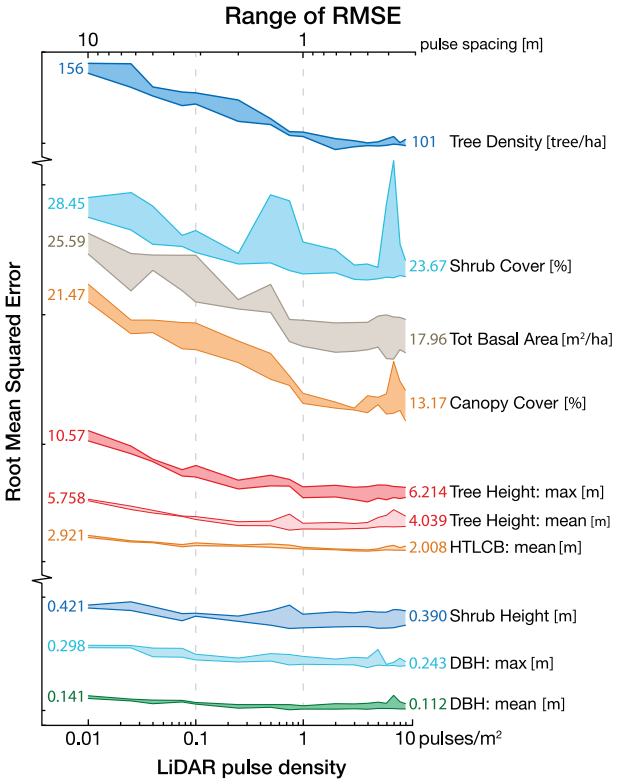

Fig. 6. Ranges of the root mean squared errors (RMSE) for all three models (MR, SVR, and GP) as a function of lidar pulse density. Pulse spacing is indicated on top. The values directly to the left and right of the ranges are the average RMSE for the minimum and maximum pulse density. Units are indicated after the metric names on the right. The y-axis is linear while the x-axes are logarithmic.

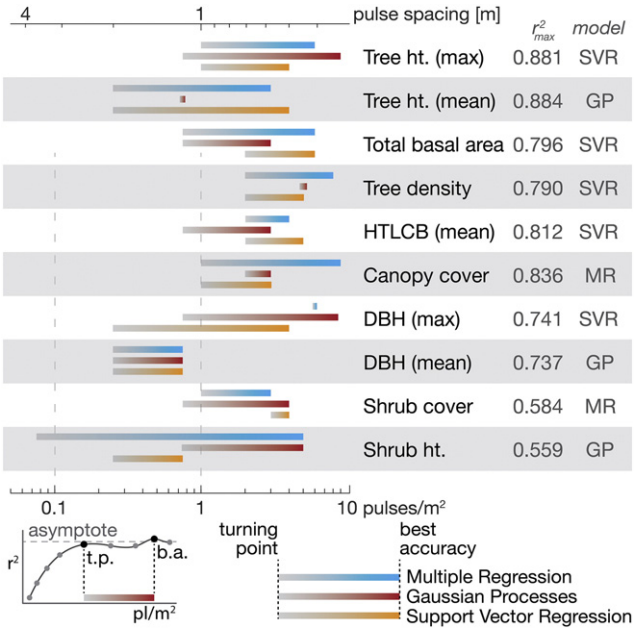

Fig. 7. Synthesis of the observed results. The horizontal colored lines indicate pulse density ranges where the accuracies were deemed reasonable for the given metric. The left end of each accuracy range corresponds to its turning point—pulse density at which the metric accuracy plateaus or is comparable to its maximum. The right end of the range marks the pulse density at which the given model yields absolute maximum correlation coefficient. The three color lines correspond to individual algorithms, in order from top: MR (blue), GP (red), and SVR (orange). The two columns on the right of each metric reflect the maximum r^2 of all three algorithms and the model used to obtain it. For example, the turning point and the best accuracy for maximum tree height were located at 1 and 6 pl/m^2, respectively; SVR predicted the metric with the highest accuracy: $r^2 = 0.881$.

require a threshold density to achieve reasonable accuracy, but that do not benefit significantly from very high lidar density. This asymptotic behavior is very clear in maximum tree height and total basal area, where the turning points are reached at 1 and 2 pl/m^2, respectively. For example, the accuracy of total basal area using SVR drops significantly below 2 pl/m^2 ($r = 0.789$), but thereafter remains approximately equal to its maximum (0.796) and the 9 pl/m^2 accuracy (0.782). Similarly, the accuracy of maximum tree height using SVR rises steadily until 1 pl/m^2 (0.860), at which point it is similar to its maximum correlation coefficient (0.869). This level of accuracy is similar to previous studies that derived tree heights using lidar pulse density of 2.6 pl/m^2 (Erdody & Moskal, 2010) and >4 pl/m^2 (Zhao et al., 2011), although our results were not as accurate, most likely due to the more complex study area.

The turning point depends on the forest metric and/or the predictive model. For tree density, canopy cover, and shrub cover, the turning point is reached at or above 1 pl/m^2 across all models. This indicates that "cover" metrics require relatively higher number of lidar returns to be mapped accurately. Conversely, mean tree height, mean DBH, and shrub height reach their turning points between 0.075 and 0.75 pl/m^2, indicating that less dense data can be used to estimate these metrics and still obtain reasonable results (we should note here that although the turning point for shrub height occurs at a very low density, that metric is predicted at an overall low accuracy level). The predictive algorithms also influence the turning point. In general, SVR outputs reliable results at lower pulse densities than MR and GP. This implies that when working with low-density data, it may be best to use SVR in order to obtain reasonable results. MR almost always requires relatively higher pulse density.

The calculated RMSE steadily increased for all metrics as the pulse density decreased. For example, the mean tree height RMSE as derived by the SVR was 3.92 and 5.67 m at 9 and 0.01 pl/m^2, respectively. The maximum tree height and maximum DBH RMSE were both higher than their corresponding mean metric RMSE. One metric, shrub cover, exhibited high outlier RMSE values at high pulse densities when estimating using the MR. The combination of relatively high RMSE with low and unstable correlation coefficient of this metric leads us to believe that MR is unsuitable for estimating shrub cover in high tree-density, mixed-conifer forest.

Although the focus of this work is not algorithm comparison, there were a few noteworthy results with regard to method. In general, the three algorithms performed similarly for most of the variables. In a few cases, the SVR or the GP yielded better results: GP outperformed SVR and MR in estimating the mean DBH, shrub height, and mean tree height, while SVR outperformed the other algorithms in estimating the maximum tree height, mean HTLCB, and tree density (Table 2). In comparison to the other algorithms, MR performed particularly poorly in estimating the mean DBH, mean tree height, and maximum DBH. The mean DBH was most significantly affected by the algorithm used, especially at pulse densities above 0.1 pl/m^2: GP outperformed SVR and MR.

MR requires the most lidar points to obtain high correlation coefficients, followed by GP and SVR. The SVR and GP were most commonly the best performers. The SVR often performed better in lower densities (maximum and mean tree height, maximum DBH, and shrub height, total basal area, and mean HTLCB), while in some cases the GP performed decidedly better in the high pulse densities (mean tree height and DBH, and shrub height). This result indicates that the use of SVR may be preferable when working with low-density lidar data (below 0.3 pl/m^2).

Overall, our results indicate that very high lidar pulse density may not be necessary to predict typical forest structure metrics at the plot scale. From the best correlation coefficients obtained by the three algorithms, five out of ten best metrics were calculated from the lowest,

Table 2
Best-performing algorithms categorized into three groups of pulse densities: low, medium, and high. The noted algorithm performed best within the given pulse density category. ~ indicates mixed results.

Forest metric	<0.1 pl/m^2	0.1–1 pl/m^2	>1 pl/m^2
Tree height (max)	SVM	SVM	MR/SVM
Tree height (mean)	SVM	GP	GP
Total basal area	SVM	~	MR/SVM
Tree Density	~	SVM	SVM
HTLCB (mean)	SVM	MR/GP	SVM
Canopy cover	~	~	MR/GP
DBH (max)	SVM/GP	SVM	SVM/GP
DBH (mean)	~	GP	GP
Shrub cover	~	SVM	SVM
Shrub height	~	GP	GP

and four were from the highest pulse density—the best-obtained correlation coefficient for each metric is indicated in Fig. 7. This finding is particularly important for land managers that need to survey a large area with a specific forest metric and accuracy in mind. Our conceptual model of the tradeoffs among cost, coverage and density (Fig. 1) can help guide this kind of process. For example, if tree height is the most important metric to estimate at a reasonable accuracy level, it may be sufficient to acquire lidar data at about 1 pl/m^2. On the other hand, if it is critical to derive the average HTLCB at a high accuracy (e.g. in a wildfire-prone forest where ladder fuels play an important role in forest dynamics), then it may be advisable to acquire a much higher pulse density—at least 2 to 4 pl/m^2. Previous research (Goodwin et al., 2006; Næsset, 2004; Takahashi et al., 2010; Thomas et al., 2006; Naesset, 2009) indicates that AGL-and therefore footprint size-affects the characteristics of the lidar point cloud and the absolute values of biophysical forest predictions; however, it has little effect on the prediction's accuracy. The studies listed here collected data at varying AGLs. It should be reiterated however that this work uses simulated lower lidar pulse densities, and not data collected from multiple missions.

Unlike most of the previous lidar forestry studies, the analyses presented in this paper were performed in a topographically complex, steep terrain covered by dense, mixed-conifer forest. For example, Tesfamichael et al. (2010) and Magnusson et al. (2007) assessed the effects of point density on a few forest metric but in a much simpler terrain and forest composition: South African rolling foothills and Sweden's low-relief coniferous forests, respectively. We expect that the derived accuracies would improve in less challenging areas. Further, all analyses were completed at the plot-scale (equivalent to a 24 m pixel size), and we would expect that the required pulse density for accurate identification and quantification of individual trees from lidar data would be larger than that required for plot-scale analysis. For plot scale analysis of forests, there might be cost savings and/or economies of scale in acquiring discrete return lidar data at lower densities.

4. Conclusions

The accuracy of predicted forest structure metrics decreases as the pulse density decreases, but it remains relatively high until low densities (e.g. 1 pl/m^2). This effect occurred with all tested predictive algorithms. The accuracy of tree height (mean and max), total basal area, DBH (mean and max), and shrub height remained *relatively* high until the pulse density decreased to 1 pl/m^2. Tree density, canopy cover, and shrub cover, and mean HTLCB typically required >1 pl/m^2. Support vector machine (SVR) and Gaussian processes (GP) algorithms consistently outperformed simple multiple regression model (MR). MR required the highest pulse density to deliver good results; SVR and GP outperformed other algorithms when the pulse density was low (<0.3 pl/m^2) and high (>1 pl/m^2), respectively. This work shows that low-density lidar data are capable of estimating the typical forest structure metrics at a plot level (~24 m pixel size) reliably. This finding indicates that land managers faced with a constrained budget may be able to cover larger areas at a lower cost when trying to estimate one of metrics tested in this work. However, higher density data are necessary for "cover" metrics and individual tree analyses.

Acknowledgments

This is SNAMP Publication #18. The Sierra Nevada Adaptive Management Project is funded by the USDA Forest Service Region 5, the USDA Forest Service Pacific Southwest Research Station, US Fish and Wildlife Service, California Department of Water Resources, California Department of Fish and Game, California Department of Forestry and Fire Protection, and the Sierra Nevada Conservancy.

Appendix A. Supplementary data

Supplementary data associated with this article can be found in the online version, at http://dx.doi.org/10.1016/j.rse.2012.11.024. These data include Google maps of the most important areas described in this article.

References

Anderson, E. S., Thompson, J. A., Crouse, D. A., & Austin, R. E. (2006). Horizontal resolution and data density effects on remotely sensed LIDAR-based DEM. *Geoderma*, *132*(3–4), 406–415.
Baltsavias, E. P. (1999). Airborne laser scanning: Basic relations and formulas. *ISPRS Journal of Photogrammetry and Remote Sensing*, *54*, 199–214.
Brandtberg, T., Warner, T. A., Landenberger, R. E., & McGraw, J. B. (2003). Detection and analysis of individual leaf-off tree crowns in small footprint, high sampling density lidar data from the eastern deciduous forest in North America. *Remote Sensing of Environment*, *85*(3), 290–303.
Chang, Y. -C., Habib, A. F., Lee, D. C., & Yom, J. -H. (2008). Automatic classification of lidar data into ground and non-ground points. *Paper presented at the ISPRS Congress Beijing 2008, Beijing, China*.
Clark, M. L., Clark, D. B., & Roberts, D. A. (2004). Small-footprint lidar estimation of sub-canopy elevation and tree height in a tropical rain forest landscape. *Remote Sensing of Environment*, *91*(1), 68–89.
Collins, B. M., Stephens, S. L., Roller, G. B., & Battles, J. J. (2011). Simulating fire and forest dynamics for a landscape fuel treatment project in the Sierra Nevada. *Forest Science*, *57*(2), 77–88.
Cunningham, R., Gisclair, D., & Craig, J. (2004). *The Louisiana statewide lidar project.* Baton Rouge, Louisiana: Louisiana State University.
Erdody, T. L., & Moskal, M. L. (2010). Fusion of LiDAR and imagery for estimating forest canopy fuels. *Remote Sensing of Environment*, *114*(4), 725–737.
Frank, E., Hall, M., Holmes, G., Kirkby, R., Pfahringer, B., Witten, I. H., et al. (2010). Weka-a machine learning workbench for data mining. *Data Mining and Knowledge Discovery Handbook* (pp. 1269–1277).
Goodwin, N. R., Coops, N. C., & Culvenor, D. S. (2006). Assessment of forest structure with airborne LiDAR and the effects of platform altitude. *Remote Sensing of Environment*, *103*(2), 140–152.
Guo, Q., Li, W., Yu, H., & Alvarez, O. (2010). Effects of topographic variability and lidar sampling density on several DEM interpolation methods. *Photogrammetric Engineering and Remote Sensing*, *76*(6), 701–712.
He, Q., & Li, N. (2012). Estimation of individual tree parameters using small-footprint LiDAR with Different density in a coniferous forest. *Advanced Materials Research*, *518–523*, 5320–5323.
Hodgson, M. E., & Bresnahan, P. (2004). Accuracy of airborne lidar-derived elevation: empirical assessment and error budget. *Photogrammetric Engineering and Remote Sensing*, *70*(3), 331–339.
Hsu, C. W., Chang, C. C., & Lin, C. J. (2003). *A practical guide to support vector classification.* Taipei, Taiwan: N.T.U. Department of Computer Science, National Taiwan University.
Isenburg, M. (2011). LAStools — efficient tools for LiDAR processing (Version 111216). Retrieved from http://lastools.org.
Jakubowski, M.K., Guo, Q., Collins, B.M., Stephens, S.L. & Kelly, M. (in press). Predicting surface fuel models and fuel metrics using lidar and CIR imagery in a dense, mountains forest. *Photogrammetric Engineering & Remote Sensing*.
Johansen, K., Phinn, S., & Witte, C. (2010). Mapping of riparian zone attributes using discrete return LiDAR, QuickBird and SPOT-5 imagery: Assessing accuracy and costs. *Remote Sensing of Environment*, *114*(11), 2679–2691.
Keerthi, S. S., Shevade, S. K., Bhattacharyya, C., & Murthy, K. R. K. (2001). Improvements to Platt's SMO algorithm for SVM classifier design. *Neural Computation*, *13*(3), 637–649.
Kohavi, R. (1995). A study of cross-validation and bootstrap for accuracy estimation and model selection. *Paper presented at the International Joint Conference on Artificial Intelligence.* Stanford University.

Liu, X., & Zhang, Z. (2008). LIDAR data reduction for efficient and high quality DEM generation. *Paper presented at the ISPRS Congress Beijing 2008, Beijing, China* (http://eprints.usq.edu.au/4569/).

Lovell, J. L., Jupp, D. L. B., Culvenor, D. S., & Coops, N. C. (2003). Using airborne and ground-based ranging lidar to measure canopy structure in Australian forests. *Canadian Journal of Remote Sensing*, *29*(5), 607–622.

Lovell, J. L., Jupp, D. L. B., Newnham, G. J., Coops, N. C., & Culvenor, D. S. (2005). Simulation study for finding optimal lidar acquisition parameters for forest height retrieval. *Forest Ecology and Management*, *214*(1–3), 398–412.

Magnussen, S., Naesset, E., & Gobakken, T. (2010). Reliability of LiDAR derived predictors of forest inventory attributes: A case study with Norway spruce. *Remote Sensing of Environment*, *114*(4), 700–712.

Magnusson, M., Fransson, J. E. S., & Holmgren, J. (2007). Effects on estimation accuracy of forest variables using different pulse density of laser data. *Forest Science*, *53*(6), 619–626.

Næsset, E. (2004). Effects of different flying altitudes on biophysical stand properties estimated from canopy height and density measured with a small-footprint airborne scanning laser. *Remote Sensing of Environment*, *91*(2), 243–255.

Naesset, E. (2009). Effects of different sensors, flying altitudes, and pulse repetition frequencies on forest canopy metrics and biophysical stands properties derived from small-footprints airborne laser data. Remote Sensing of Environment, 113(1), 148–159.

Olsen, R. C., Puetz, A. M., & Anderson, B. (2009). Effects of lidar point density on bare earth extraction and DEM creation. *Paper presented at the American Society for Photogrammetry and Remote Sensing Baltimore 2009, Baltimore, Maryland*.

Pirotti, F., & Tarolli, P. (2010). Suitability of LiDAR point density and derived landform curvature maps for channel network extraction. *Hydrological Processes*, *24*(9), 1187–1197.

Rasmussen, C. (2004). Gaussian processes in machine learning. In O. Bousquet, U. von Luxburg, & G. Rätsch (Eds.), *Advanced lectures on machine learning*, *Vol. 3176*. (pp. 63–71) Berlin: Springer.

Sanii, S. (2008). *Assessing the effect of point density and terrain complexity on the quality of LiDAR-derived DEMs in multiple resolutions.* Masters of geographic information systems masters. Calgary, Alberta, Canada: University of Calgary.

Smola, A., & Schölkopf, B. (2004). A tutorial on support vector regression. *Statistics and Computing*, *14*(3), 199–222.

Soininen, A. (2012). *Terra scan for microstation, user's guide (Version 132)*. Jyvaskyla, Finland: Terrasolid Ltd.

Stephens, S. L., & Collins, B. M. (2004). Fire regimes of mixed conifer forests in the north-central Sierra Nevada at multiple spatial scales. *Northwest Science*, *78*(1), 12–23.

Takahashi, T., Awaya, Y., Hirata, Y., Furuya, N., Sakai, T., & Sakai, A. (2008). Effects of flight altitude on LiDAR-derived tree heights in mountainous forests with poor laser penetration rates. *Photogrammetric Journal of Finland*, *21*(1), 86–96.

Takahashi, T., Awaya, Y., Hirata, Y., Furuya, N., Sakai, T., & Sakai, A. (2010). Stand volume estimation by combining low laser-sampling density LiDAR data with QuickBird panchromatic imagery in closed-canopy Japanese cedar (*Cryptomeria japonica*) plantations. *International Journal of Remote Sensing*, *31*(5), 1281–1301.

Tesfamichael, S. G., van Aardt, J. A. N., & Ahmed, F. (2010). Estimating plot-level tree height and volume of *Eucalyptus grandis* plantations using small-footprint, discrete return lidar data. *Progress in Physical Geography*, *34*(4), 515–540.

Thomas, V., Treitz, P., McCaughey, J. H., & Morrison, I. (2006). Mapping stand-level forest biophysical variables for a mixedwood boreal forest using lidar: an examination of scanning density. *Canadian Journal of Forest Research*, *36*(1), 34–47.

Tilley, B. K., Munn, I. A., Evans, D. L., Parker, R. C., & Roberts, S. D. (March 14–16). Cost considerations of using LiDAR for timber inventory. *Paper presented at the Southern Forest Economics Workshop, St. Augustine, Florida*.

Veneziano, D., Hallmark, S., & Souleyrette, R. (2002). Comparison of lidar and conventional mapping methods for highway corridor studies. *Final Report*. Ames, Iowa: Center for Transportation Research and Education, Iowa State University.

Wulder, M. A., White, J. C., Coops, N. C., & Butson, C. R. (2008). Multi-temporal analysis of high spatial resolution imagery for disturbance monitoring. *Remote Sensing of Environment*, *112*(6), 2729–2740.

Zhao, K., Popescu, S., Meng, X., Pang, Y., & Agca, M. (2011). Characterizing forest canopy structure with lidar composite metrics and machine learning. *Remote Sensing of Environment*, *115*(8), 1978–1996.